

Study on Electrochemical and Magnetic Properties of CoNi Alloy Coating Electrodeposited on Semiconductor Silicon

Shuli Yi*, Chengbo Yin, Hongli Lin, Xiujuan Leng

Qingdao Huanghai University, Qingdao, Shandong, 266427, China

*E-mail: ysl_pro_qdedu@126.com

Received: 12 May 2022 / Accepted: 3 June 2022 / Published: 4 July 2022

The Co-Ni coating on the surface of semiconductor silicon commonly used for computer fields is prepared by plating using solutions containing different concentrations of cobalt sulfate. The influence of cobalt ions on the electrochemical and magnetic properties of Co-Ni coating is investigated to reveal the internal relationship of magnetic property, surface morphology and microstructure. The electrodeposition of cobalt is a diffusion controlled instantaneous nucleation while the electrodeposition of nickel belongs to an electrochemical controlled continuous nucleation. Increasing the concentration of cobalt sulfate in the plating solution from 5 g/L to 20 g/L is beneficial to increase the cobalt content and thickness, refine the particle size and reduce the surface roughness of Co-Ni coating, so as to increase the magnetic property. However, when the cobalt sulfate in the plating solution is 40 g/L, higher concentration of cobalt ions makes a large number of cobalt hydroxide and oxide adsorbed on the cathode surface resulting in poor magnetic property. The Co-Ni coating electrodeposited on the condition of 30 g/L cobalt sulfate has the best magnetic property with 314.64 Oe coercivity and 102.50 emu/g saturation magnetization.

Keywords: Co-Ni coating; Computer fields; Electrodeposition; Magnetic property;

1. INTRODUCTION

Magnetic materials refer to the materials composed of transition elements such as iron, cobalt, nickel and their alloys, which can produce magnetism directly or indirectly. According to the strength of magnetic properties, magnetic materials are mainly divided into permanent magnetic materials and soft magnetic materials [1-5]. Meanwhile, soft magnetic materials are widely used in the computer fields. For example, soft magnetic filters, chip magnetic bead filters and soft magnetic shields are frequently used to minimize the noise generated by the interaction of computer power cables and electronic devices. In order to read computer data efficiently, the magnetic head of reading data is often made of soft magnetic coating [6-8]. Moreover, a large number of soft magnetic coatings are

prepared on the surface of silicon inside the computer device, which makes the computer device more miniaturized, higher performance and lower electromagnetic noise. The common soft magnetic coating includes Fe-Ni coating, Co-Ni coating, Fe-Co coating and so on [9-14]. Many preparation methods reported can be used to obtain soft magnetic coating. Meanwhile, electrodeposition method has many advantages, such as strong stability, low cost, easy operation and so on. The Co-Ni based electrodeposited coatings have received extensive attentions for their excellent magnetic properties [15-17]. The cobalt content in the Co-Ni coating will affect the surface morphology and structure that contributes directly to the magnetic property. Some methods can change the cobalt content in the Co-Ni coating during electrodeposition, such as adding different complexing agents, changing the deposition potential and so on. Since the electrodeposition of cobalt belongs to a diffusion control, increasing the content of cobalt in the bath is beneficial to accelerate the mass transfer rate of cobalt ion, and thus increase the content of cobalt in the coating. However, if the concentration of cobalt ions in the solution is high, a large amount of cobalt oxides and hydroxides are easily precipitated on the cathode surface, which is not conducive to improving the magnetic properties of the coating. Therefore, by changing the concentration of cobalt ion in the plating solution, this paper studies the influence of cobalt ion concentration on the thickness, roughness, morphology, structure and magnetic properties of the electrodeposited Co-Ni coating, and further reveals the internal relationship of magnetic properties, morphology and structure, which has a certain innovation.

2. EXPERIMENTAL

2.1 Chemical agents and plating conditions

The chemical agents and plating conditions of Co-Ni electrodeposited coating on semiconductor silicon is listed in Table 1 below.

Table 1. Chemical agents and plating conditions of Co-Ni electrodeposited coating

Chemical agent and conditions	Concentration and parameter
CoSO ₄ ·7H ₂ O	5~40 g/L
NiSO ₄ ·6H ₂ O	20 g/L
C ₆ H ₁₄ N ₂ O ₇	100 g/L
H ₃ BO ₃	20 g/L
Na ₂ SO ₄	30 g/L
Current density	1.5 A/dm ²
Temperature	50 °C
Plating time	60 min
pH	6

For table 1, it is known that the CoSO₄ and NiSO₄ are chosen as the main salts during the Co-Ni coating electrodeposition to offer cobalt and nickel ions. Ammonium citrate is as the complexing

agent in the plating solution. The boric acid and sodium sulfate are as the buffering agent the conductive salt respectively. The pH value of the solution is adjusted to 6 using sodium hydroxide or dilute sulfuric acid. The plating time is 60 min at the temperature of 50 °C.

2.2 Preparation of Co-Ni electrodeposited coating

The surface area of the semiconductor silicon is 2 cm×2 cm which is used as the substrate to be electrodeposited Co-Ni coating. The substrate should be pretreated before plating, which is firstly cleaned by the mixed solution with acetone and ethanol (1:1). After the substrate is cleaned by pure water, it is immersed into the acid solution containing 68% nitric acid and 40% hydrofluoric acid (1:2). Finally, the substrate is washed by pure water and dried. The 100 ml plating aqueous solution is prepared based on the information listed in Table 1. The prepared electroplating solution needs to be placed for 24 hours to ensure that metal ions and complexing agent are fully complexed. The pure platinum plate (3 cm×3 cm) is as the counter electrode and the silver-silver chloride electrode is as the reference electrode. The Co-Ni coating is obtained on the surface of silicon by electrodeposition from 100 ml plating solution with 1.5 A/dm² current density at 50 °C for 60 minutes. The concentration of cobalt sulfate is changed from 5 g/L to 40 g/L to investigate the effect of cobalt ions concentration on the surface morphology, structure and magnetic property of Co-Ni coating.

2.3 Testing method

Cyclic voltammetry and current-time curves of Co-Ni co-deposition are analyzed by Princeton Parstat 2273 electrochemical station to investigate the nucleation mechanism. The silicon substrate (1 cm×1 cm) is the working electrode, the pure platinum plate (3 cm×3 cm) is as the counter electrode and the silver-silver chloride electrode is chosen as the reference electrode. For the cyclic voltammetry curve, the potential range is -1.4 V~0.3 V with 10 mV/s scanning rate. For the current-time curve, the deposition potential is -1.4 V for 200 s. The roughness and thickness of the Co-Ni electrodeposited coating is measured by surface profiler SP2100V with 10 μm/s and 1 μm/s scanning rate respectively. X-ray diffraction (Miniflex 600) and energy dispersive spectrometer (EDX3600) are used to characterize the structure and composition of Co-Ni electrodeposited coating respectively. Finally, the magnetic property of Co-Ni coating is evaluated by vibration sample magnetometer (Lakeshore 7400) from 1.5 T to -1.5 T.

3. RESULTS AND DISCUSSION

3.1 Cyclic voltammetry curves of Co-Ni electrodeposited coating

As can be seen in Figure 1, the initial deposition potential of cobalt is around -0.33 V. When the potential is more negative than -0.33 V, the cathode current starts to increase gradually indicating that cobalt starts to be deposited slowly. However, when the potential is more negative than -0.88 V,

the cathode current increases extremely which means that the deposition of cobalt is dominant and fast. As the electrodeposition of cobalt is controlled by diffusion, the mass transfer rate of cobalt in solution is the smallest. As the electrochemical reaction goes on, the concentration of cobalt ions near the cathode surface is far less than that in the solution.

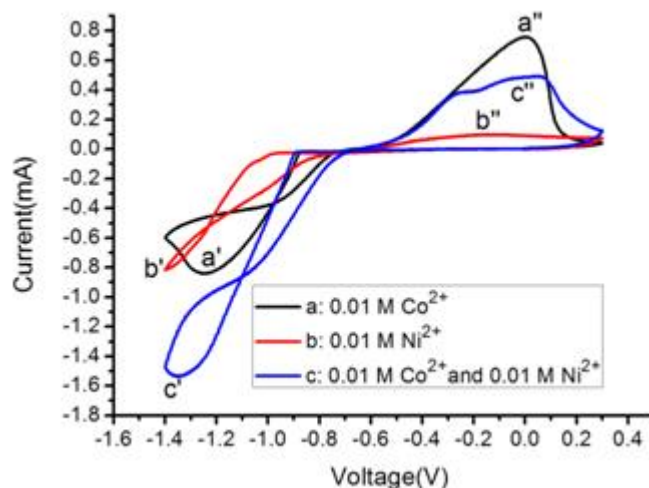
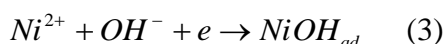
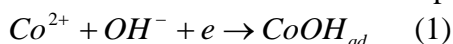


Figure 1. Cyclic voltammetry of silicon in different plating solutions: a. 0.01 M Co^{2+} ; b. 0.01 M Ni^{2+} ; c. 0.01 M Co^{2+} and 0.01 M Ni^{2+} ; The potential range is -1.4 V~0.3 V with 10 mV/s scanning rate; The reference electrode is silver-silver chloride electrode.

At this time, with the deposition potential increases, the cathode current gradually decreases forming a typical reduction peak at -1.25 V (a'). The initial deposition potential of nickel is around -0.308 V which is more positive than that of cobalt. It is found out that because the electrodeposition of nickel belongs to an electrochemical control process, there is no obvious reduction peak found on the cyclic voltammetry of nickel. The co-deposition of Co-Ni starts at the potential of -0.434 V which is more negative than that of cobalt and nickel indicating that co-deposition of Co-Ni needs higher overpotential. The typical reduction peak of Co-Ni co-deposition can be observed at the potential of -1.34 V (c') which is more negative than that of cobalt (a'). Moreover, the dissolution potential of CoNi (c'') is between that of cobalt (a'') and nickel (b'').

The co-deposition mechanism of Co-Ni can be explained by the following equations [18-19].



From the equations, the electrodeposition of Co and Ni can be divided into two steps. The pH value increases during the plating process will form CoOH^+ and NiOH^+ mixed with the complexing agent to generate CoOH_{ad} and NiOH_{ad} which will get electrons to be reduced to cobalt and nickel.

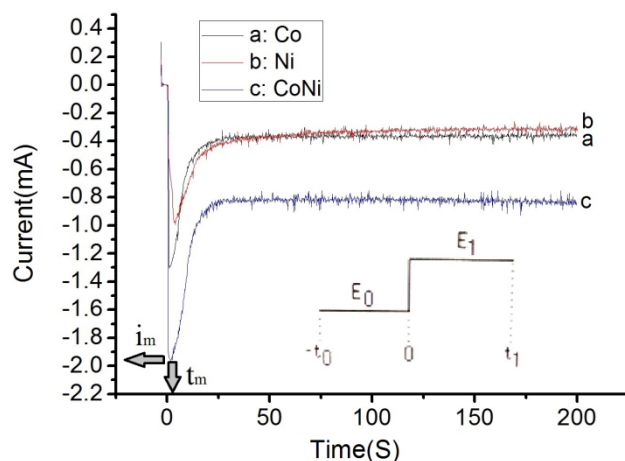


Figure 2. The current-time curve of silicon in different solutions: a. 0.01 M Co^{2+} ; b. 0.01 M Ni^{2+} ; c. 0.01 M Co^{2+} and 0.01 M Ni^{2+} ; The E_0 is 0 V, the E_1 is -1.4 V, t_0 is 3 s and t_1 is 200 s. The reference electrode is silver-silver chloride electrode.

According to Figure 2, as the increase of time, the cathode current of silicon in Co, Ni and CoNi solution all increases to a maximum value and then decrease to a constant value. At the beginning of electrodeposition, the metal particles nucleate and grow up on the cathode surface, which increase the current distribution on the cathode surface resulting in the increase of current intensity on the cathode surface. As the reaction progresses, the cathode surface are uniformly covered with metal particles and the thickness of diffusion layer increases. Finally, the deposition current gradually decreases to reach a constant value. The electrochemical parameters of current-time curve are listed in Table 2.

Table 2. Electrochemical parameters of current-time curves

Solution(M)	Potential(V)	Time(s)	i_m (mA)	t_m (s)	i_c (mA)
0.01 Co^{2+}	-1.4 V	200	1.31	1.13	0.36
0.01 Ni^{2+}	-1.4 V	200	0.99	4.02	0.31
0.01 Co^{2+} +0.01 Ni^{2+}	-1.4 V	200	1.96	1.75	0.84

The i_m is the maximum value of current while the t_m is the time used to get the i_m . And, the i_c is the current at which the electrodeposition reaches equilibrium. The i_m and t_m are two important parameters which determine the nucleation mechanism during the initial of electrodeposition. Two nucleation models can be used to characterize the nucleation mechanism: continuous nucleation and instantaneous nucleation. The instantaneous nucleation is that crystal nuclei are generated at the activation points on the substrate surface at the initial stage of electrodeposition. Continuous nucleation requires an induction period, and the nucleation process is related to time. The type of nucleation can be determined using the classical Scharifker equation described as follows:

$$\text{Instantaneous nucleation} \quad \frac{i^2(t)}{i_m^2} = \frac{1.9542}{t/t_m} \left\{ 1 - \exp \left[-1.2564 \left(\frac{t}{t_m} \right) \right] \right\}^2 \quad (5)$$

$$\text{Continuous nucleation} \quad \frac{i^2(t)}{i_m^2} = \frac{1.2254}{t/t_m} \left\{ 1 - \exp \left[-2.3367 \left(\frac{t}{t_m} \right) \right] \right\}^2 \quad (6)$$

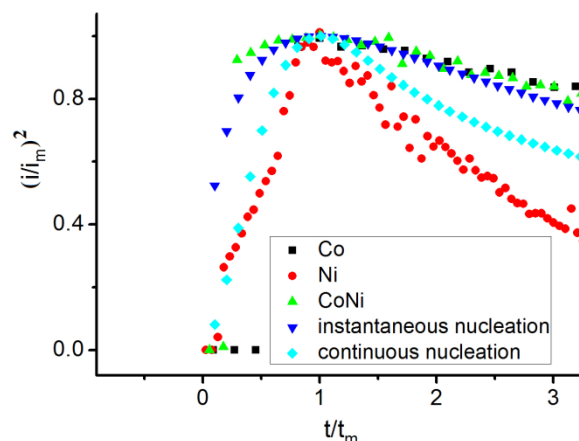


Figure 3. The $(i/i_m)^2$ vs t/t_m curves for electrodeposition of Co, Ni and CoNi alloy coatings compared to instantaneous and continuous nucleation curve

According to the data combined with Table 2 and Figure 3, it is obvious that the nucleation mechanism of Co and CoNi is instantaneous nucleation and Ni nucleation belongs to continuous nucleation. The nucleation mechanism of cobalt and nickel has been reported by many researchers who indicate that the temperature and substrate may also affect the nucleation mechanism of metal [20-23].

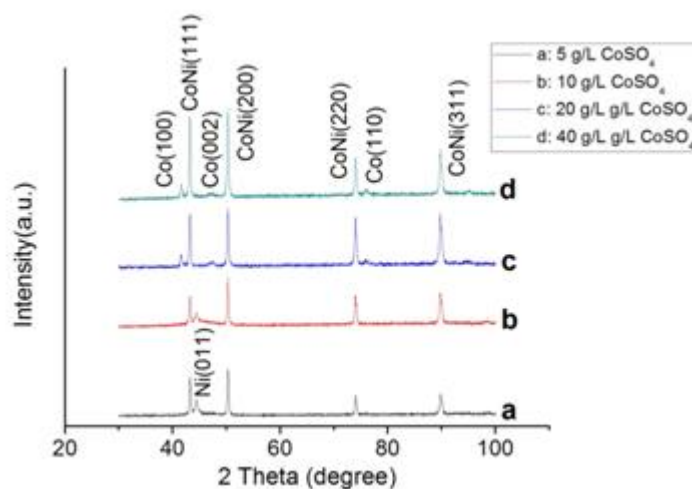
3.2 Composition and microstructure of CoNi electrodeposited coating

According to previous analysis, the electrodeposition of cobalt belongs to a diffusion controlled instantaneous nucleation, and the electrodeposition of nickel belongs to an electrochemical controlled continuous nucleation. Compared with nickel ions, the mass transfer rate of cobalt ions in the bath is slower, resulting in lower cobalt content in the Co-Ni coating, which is not conducive to improving the magnetic properties of Co-Ni coating. Therefore, the paper is aim to improve the cobalt content in Co-Ni alloy by changing the concentration of cobalt ions in the plating solution, and reveals the direct internal relationship between cobalt content, morphology, microstructure and magnetic properties. The effect of cobalt sulfate concentration in the plating solution on the composition of Co-Ni coating is listed in Table 3.

Table 3. Composition of Co-Ni coating electrodeposited from solutions with different concentrations of cobalt sulfate

Concentration of CoSO ₄ (g/L)	Percentage of cobalt (%)	Percentage of nickel (%)
5	13.7	86.3
10	24.6	75.4
20	42.2	57.8
40	53.1	46.9

According to the Table 3, when the content of cobalt sulfate in the plating solution is 5 g/L, the content of cobalt and nickel in the Co-Ni coating is 13.7% and 86.3%, respectively. As the electrodeposition of cobalt is controlled by diffusion, its mass transfer rate is less than that of nickel, resulting in low cobalt content in the Co-Ni coating. Moreover, with the progress of electrodeposition, the hydrogen evolution near cathode leads to the increase of pH value, and the nickel hydroxide hydrate generated will further hinder the diffusion process of cobalt ions, thus reducing the cobalt content in the coating. However, when the content of cobalt sulfate increases from 5 g/L to 40 g/L, the cobalt content increases gradually while the amount of nickel decreases dramatically. It can be seen that increasing the concentration of cobalt ion in the plating solution is beneficial to increase the content of cobalt in the coating, thus reducing the content of nickel in the coating.

**Figure 4.** XRD patterns of Co-Ni coating electrodeposited from solutions with different concentrations of cobalt sulfate. The scanning angle is from 30° to 100° and the scanning rate is 5°/min.

XRD patterns are used to analyze the microstructure of different Co-Ni coatings, and the results are shown in Figure 4. The XRD patterns of CoNi alloy coatings prepared from solution containing different concentrations of cobalt sulfate show very strong diffraction peaks and very good crystallinity, which belongs to the typical crystal structure [24]. Co-Ni alloy coating has four basic diffraction peaks, which are CoNi(111), CoNi(200), CoNi(220) and CoNi(311). For example,

Thanikaikarasan investigates the structure of Co-Ni alloy coating electrodeposited on copper substrate which is similar to the structure of Co-Ni alloy coating prepared in the paper [25]. With the increase of the concentration of cobalt ion in the plating solution, the diffraction peak of CoNi increases gradually and the crystallinity of CoNi increases. It is mainly attributed to that increasing the concentration of cobalt ions in the plating solution is conducive to increasing the mass transfer rate of cobalt, thus increasing the deposition rate and deposition quality of Co-Ni coating. When the content of cobalt sulfate in the bath is 5 g/L, the diffraction peak of Ni(011) can be observed on the XRD pattern. The diffraction peaks of Co(100), Co(002) and Co(110) are enhanced with the increase of cobalt ions in the bath, which indicates that some cobalt metals are electrodeposited independently.

3.3 Thickness and roughness of CoNi electrodeposited coating

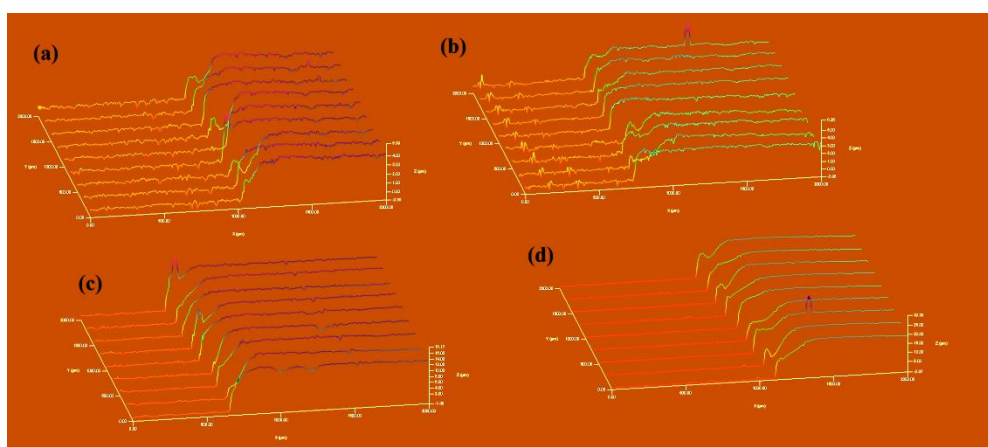


Figure 5. Thickness of Co-Ni coating electrodeposited from solutions with different concentrations of cobalt sulfate: (a) 5 g/L; (b) 10 g/L; (c) 20 g/L; (d) 40 g/L; The scanning range is 2000 $\mu\text{m} \times 2000 \mu\text{m}$ at the scanning rate 10 $\mu\text{m/s}$.

Figure 5 shows the thickness of different Co-Ni coatings. In order to ensure the accuracy of the data, the profilometer is used to scan from the silicon substrate to the Co-Ni coating surface, and the average value of nine curves is tested to calculate the thickness of the coating listed in Table 4.

Table 4. Thickness of different Co-Ni electrodeposited coatings

Concentration of CoSO_4 (g/L)	Maximum thickness (μm)	Minimum thickness (μm)	Average thickness (μm)
5	5.39	4.23	5.08
10	6.26	5.02	6.13
20	18.17	13.94	15.24
40	30.19	19.39	21.49

It can be seen from Table 4 that the thickness of Co-Ni coating increases gradually with the increase of cobalt sulfate concentration in the plating solution. When the concentration of cobalt sulfate increases from 5 g/L to 40 g/L, the average thickness of Co-Ni coating increases from 5.08 μm to 21.49 μm . It can be seen that increasing the concentration of cobalt sulfate in the plating solution is beneficial to increase the thickness of Co-Ni alloy coating. It is mainly because cobalt belongs to a diffusion control, increasing the concentration of cobalt ion in the bath is beneficial to reduce concentration polarization, improve the mass transfer rate of cobalt ion and increase the content of cobalt in the Co-Ni coating, so as to greatly increase the thickness of the coating. The relationship between mass transfer and concentration polarization is studied in many published papers [26-28].

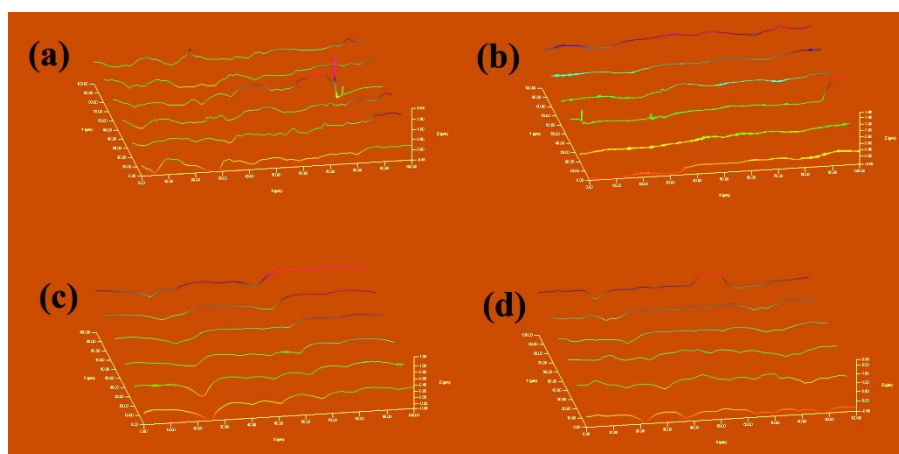


Figure 6. Roughness of Co-Ni coating electrodeposited from solutions with different concentrations of cobalt sulfate: (a) 5 g/L CoSO_4 , $R_a=0.642 \mu\text{m}$; (b) 10 g/L CoSO_4 , $R_a=0.482 \mu\text{m}$; (c) 20 g/L CoSO_4 , $R_a=0.282 \mu\text{m}$; (d) 40 g/L CoSO_4 , $R_a=0.964 \mu\text{m}$; The scanning range is $100 \mu\text{m} \times 100 \mu\text{m}$ at the scanning rate $1 \mu\text{m/s}$.

The roughness of different Co-Ni coating is shown in Figure 6. The data of six scanning curves are averaged to calculate the roughness. It can be seen that, as the increase of cobalt sulfate concentration in the plating solution from 5 g/L to 40 g/L, the roughness of Co-Ni coating is ranged from 0.282 μm to 0.964 μm . According to the XRD pattern, the Co-Ni coating obtained from the plating solution with 5 g/L cobalt sulfate has nickel diffraction peak. The nickel precipitated on the Co-Ni coating surface increase the roughness. With the increase of the concentration of cobalt sulfate in the plating solution, the diffraction peaks and crystallinity of Co-Ni alloy increases, resulting in the decrease of roughness. When the concentration of cobalt sulfate in the bath is 40 g/L, a large amount of cobalt hydroxide and cobalt oxide are precipitated near the cathode due to excessive cobalt ions, which attributes to the obvious decrease of Co-Ni coating.

3.4. Surface morphology and magnetic property of CoNi electrodeposited coating

As shown in Figure 7(a), Co-Ni coating prepared at 5 g/L cobalt sulfate has a rough surface and is composed of strip and nodular particles of different sizes.

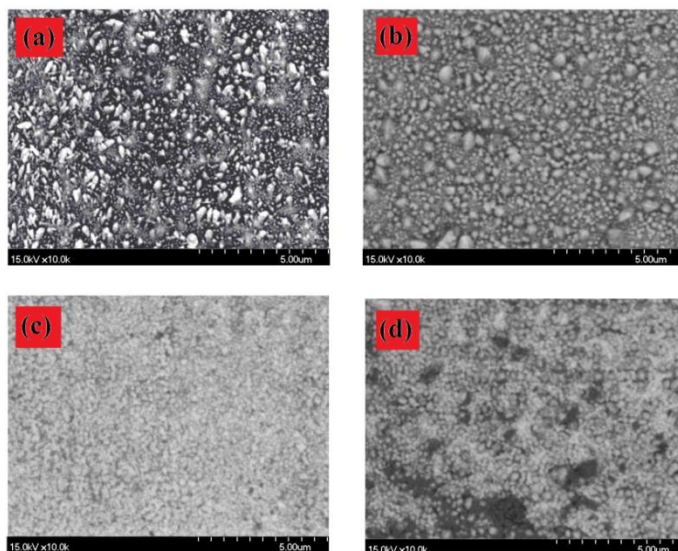


Figure 7. Surface morphology of Co-Ni coating electrodeposited from solutions with different concentrations of cobalt sulfate: (a) 5 g/L; (b) 10 g/L; (c) 20 g/L; (d) 40 g/L; The acceleration voltage is 15 kV with 10.0 k magnification times.

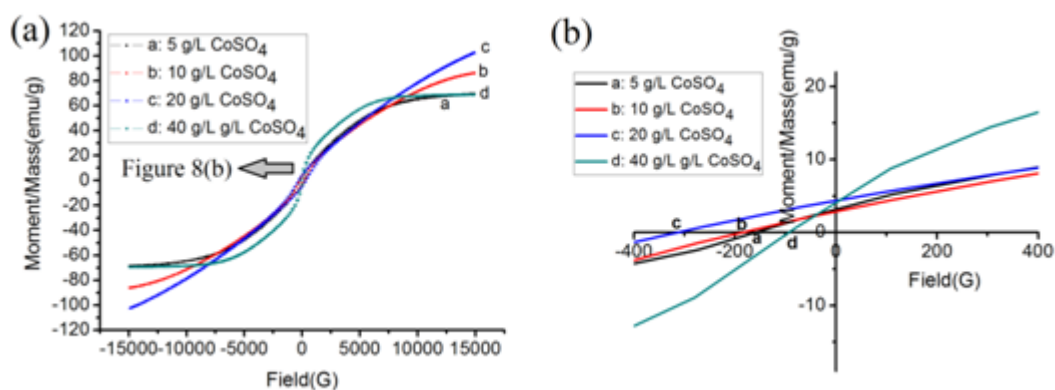


Figure 8. Vibration sample magnetometer curves of Co-Ni coating electrodeposited from solutions with different concentrations of cobalt sulfate: (a) 5 g/L; (b) 10 g/L; (c) 20 g/L; (d) 40 g/L; The applied magnetic field is from 1.5 T to -1.5 T.

The morphology of CoNi electrodeposited coatings has been reported by some authors, who point out that CoNi-fcc structure generally presents granular morphology and CoNi-hcp structure generally shows strip particle morphology [29-30]. As the concentration of cobalt ion is lower than that of nickel ion, a large amount of nickel with hexagonal structure is deposited on the surface of Co-Ni coating. With the increase of the concentration of cobalt sulfate in the plating solution, the surface

particles of Co-Ni coating are gradually refined, from strip particles to nodular particles, and the roughness decreases. When the concentration of cobalt sulfate in the plating solution is 40 g/L, the high concentration of cobalt ions makes a large number of cobalt hydroxide and oxide adsorbed on the cathode surface, and the surface of the coating becomes black and rough.

Table 5. Magnetic property of Co-Ni electrodeposited coatings

Concentration of CoSO ₄ (g/L)	Coercivity (Oe)	Saturation magnetization (emu/g)
5	161.30	69.48
10	184.66	86.15
20	314.64	102.50
40	102.67	69.01

The magnetic properties of different Co-Ni coatings are shown in Figure 8 and Table 5. Along with the increase of cobalt ions in the plating solution, the coercivity and saturation magnetization of Co-Ni coating both increase obviously. According to the above analysis, increasing the concentration of cobalt ions in the plating solution can reduce the surface roughness of the alloy, enhance the crystallinity of the alloy, and obtain Co-Ni coating with dense nodular particle, which is conducive to improving the coercivity. The relationship between grain size and coercivity is reported in some works [31-32]. In addition, increasing the concentration of cobalt ions in the plating solution can also increase the thickness and cobalt content of the alloy, so as to improve the saturation magnetization. However, when the concentration of cobalt sulfate in the plating solution is 40 g/L, the surface roughness of the Co-Ni coating is greatly increased due to the precipitation of a large number of cobalt oxides and hydroxides on the cathode, which leads to the decrease of the surface compactness and the decline of coercivity and saturation magnetization.

4. CONCLUSIONS

The Co-Ni coating is electrodeposited from plating solutions with different concentrations of cobalt sulfate. The effect of cobalt ion concentration on the thickness, roughness, morphology, microstructure and magnetic property of the electrodeposited Co-Ni coating is studied to reveal the internal relationship of magnetic property, morphology and microstructure.

(1) The electrodeposition of cobalt belongs to a diffusion controlled instantaneous nucleation, and the electrodeposition of nickel belongs to an electrochemical controlled continuous nucleation. When the concentration of cobalt sulfate in the plating solution increases from 5 g/L to 20 g/L, the thickness and cobalt content of Co-Ni coating increase simultaneously while the roughness of Co-Ni coating decreases due to the improvement of mass transfer rate of cobalt ions.

(2) CoNi alloy coatings prepared from solution containing different concentrations of cobalt sulfate show very strong diffraction peaks and very good crystallinity. With the increase of the

concentration of cobalt sulfate in the plating solution, the surface particles of Co-Ni coating are gradually refined, from strip particles to nodular particles, resulting in better coercivity and saturation magnetization. However, when the concentration of cobalt sulfate in the plating solution is 40 g/L, the high concentration of cobalt ions makes a large number of cobalt hydroxide and oxide adsorbed on the cathode surface, and the surface of the coating becomes black and rough.

References

1. Z. J. Su, W. Hou, J. Wang, Y. B. Zhang and T. Jiang, *J. Alloys compd.*, 902 (2022) 163731.
2. D. Goll, D. Schuller, G. Martinek, T. Kunert, J. Schurr, C. Sinz, T. Schubert, T. Bernthaler, H. Riegel and G. Schneider, *Addit. Manuf.*, 27 (2019) 428.
3. G. Y. Ouyang, X. Chen, Y. F. Liang, C. Macziewski and J. Cui, *J. Magn. Magn. Mater.*, 481 (2019) 234.
4. G. Weir, J. Leveneur and N. Long, *J. Magn. Magn. Mater.*, 551 (2022) 169103.
5. Q. Z. Jiang and Z. C. Zhong, *J. Mater. Sci. Technol.*, 33 (2017) 1087.
6. T. Tanaka, J. Matsuzaki, H. Kurisu and S. Yamamoto, *J. Magn. Magn. Mater.*, 320 (2008) 2931.
7. T. Osaka, *Electrochim. Acta*, 44 (1999) 3885.
8. O. Muthsam, F. Slanovc, C. Vogler and D. Suess, *J. Magn. Magn. Mater.*, 514 (2020) 167125.
9. S. Takanosu, T. Abe, Y. Yoneyama, N. Fujiwara and K. Shinagawa, *J. Magn. Magn. Mater.*, 272 (2004) 2285.
10. S. Thanikaikarasan, T. Mahalingam, T. Ahamad and S. M. Alshehri, *J. Saudi Chem. Soc.*, 24 (2020) 955.
11. M. Mohanta, S. K. Parida, A. Sahoo, Z. Hussain, M. Gupta, V. R. Reddy and V. R. R. Medicherla, *Physica B*, 572 (2019) 105.
12. A. V. Svalov, A. Larranaga and G. V. Kurlyandskaya, *Mater. Sci. Eng., B*, 188 (2014) 102.
13. Y. H. Ma, G. J. Li, J. H. Wang, Y. Zhao, K. Wang and Q. Wang, *Mater. Des.*, 111 (2016) 17.
14. A. N. Pohorilyi, A. F. Kravets, E. V. Shypil, D. Y. Podyalovsky, A. Y. Vovk, C. S. Kim, M. V. Prudnikova and H. R. Khan, *Thin Solid Film*, 423 (2003) 218.
15. S. Thanikaikarasan, R. Kanimozhi, M. Saravannan and R. Perumal, *Mater. Today: Proc.*, 46 (2021) 10248.
16. P. Cojocar, M. Spreafico, E. Gomez, E. Valles and L. Magagnin, *Surf. Coat. Technol.*, 205 (2010) 195.
17. H. Kockar, O. Demirbas, H. Kuru, M. Alper, O. Karaagac, M. Hacıismailoglu and E. Ozergin, *J. Magn. Magn. Mater.*, 360 (2014) 148.
18. Q. S. Chen, Z. Y. Zhou, G. C. Guo and S. G. Sun, *Electrochim. Acta*, 113 (2013) 694.
19. M. C. Esteves, P. T. A. Sumodjo and E. J. Podlaha, *Electrochim. Acta*, 56 (2011) 9082.
20. M. P. Pardave, J. A. Gonzalez, L. E. Botello, E. M. A. Estrada, M. T. R. Silva, J. Mostany and M. R. Romo, *Electrochim. Acta*, 241 (2017) 162.
21. A. Sahari, A. Azizi, N. Fenineche, G. Scherber and A. Dinia, *Mater. Chem. Phys.*, 108 (2008) 345.
22. S. Katnagallu, S. Vernier, M. A. Charpagne, B. Gault, N. Bozzole and P. Kontis, *Scr. Mater.*, 191 (2021) 7.
23. V. Repain, G. Baudot, H. Ellmer and S. Rousset, *Mater. Sci. Eng., B*, 96 (2002) 178.
24. O. Ergeneman, K. M. Sivaraman, S. Pane, E. Pellicer, A. Teleki, A. M. Hirt, M. D. Baro and B. J. Nelson, *Electrochim. Acta*, 56 (2011) 1399.
25. S. Thanikaikarasan, T. Mahalingam, T. Ahamad and S. M. Alshehri, *J. Saudi Chem. Soc.*, 24 (2020) 955.
26. Y. H. Xiao, H. J. Xu and C. Y. Zhao, *Int. Commun. Heat Mass Transfer*, 126 (2021) 105396.
27. Y. L. Gao, F. H. Qiao, J. Y. You, C. Shen, H. Zhao, J. L. Gu, Z. Y. Ren, K. Y. Xie and B. Q. Wei, *J. Energy Chem.*, 55 (2021) 580.

28. J. V. Arenas, M. Pritzker and M. Fowler, *Electrochim. Acta*, 89 (2013) 717.
29. P. Cojocaru, L. Magagnin, E. Gomez and E. Valles, *J. Alloys Compd.*, 503 (2010) 454.
30. J. Vilana, E. Gomez and E. Valles, *Appl. Surf. Sci.*, 360 (2016) 816.
31. H. S. Amin, T. Ohkubo, M. Gruber, T. Schrefl and K. Hono, *Scr. Mater.*, 89 (2014) 29.
32. D. S. Xue, G. Z. Chai, X. L. Li and X. L. Fan, *J. Magn. Magn. Mater.*, 320 (2008) 1541.

© 2022 The Authors. Published by ESG (www.electrochemsci.org). This article is an open access article distributed under the terms and conditions of the Creative Commons Attribution license (<http://creativecommons.org/licenses/by/4.0/>).